Cell

Meiotic Proteins Bqt1 and Bqt2 Tether Telomeres to Form the Bouquet Arrangement of Chromosomes

Yuji Chikashige,[1,2] Chihiro Tsutsumi,[1] Miho Yamane,[1] Kasumi Okamasa,[1] Tokuko Haraguchi,[1,2] and Yasushi Hiraoka[1,2,*]
[1] Cell Biology Group and CREST Research Project, Kansai Advanced Research Center, National Institute of Information and Communications Technology, 588-2 Iwaoka, Iwaoka-cho, Nishi-ku, Kobe 651-2492, Japan
[2] Department of Biology, Graduate School of Science, Osaka University, 1-1 Machikaneyama, Toyonaka, 560-0043, Japan
*Contact: yasushi@nict.go.jp
DOI 10.1016/j.cell.2006.01.048

SUMMARY

In many organisms, meiotic chromosomes are bundled at their telomeres to form a "bouquet" arrangement. The bouquet formation plays an important role in homologous chromosome pairing and therefore progression of meiosis. As meiotic telomere clustering occurs in response to mating pheromone signaling in fission yeast, we looked for factors essential for bouquet formation among genes induced under mating pheromone signaling. This genome-wide search identified two proteins, Bqt1 and Bqt2, that connect telomeres to the spindle-pole body (SPB; the centrosome equivalent in fungi). Neither Bqt1 nor Bqt2 alone functions as a connector, but together the two proteins form a bridge between Rap1 (a telomere protein) and Sad1 (an SPB protein). Significantly, when both Bqt1 and Bqt2 are ectopically expressed in mitotic cells, they also form a bridge between Rap1 and Sad1. Thus, a complex including Bqt1 and Bqt2 is essential for connecting telomeres to the SPB.

INTRODUCTION

Meiosis is a process of general importance for sexually reproducing eukaryotic organisms, generating haploid gametes from a diploid cell. This is accomplished by two consecutive rounds of chromosome segregation following one round of DNA replication. In this process, pairing and recombination of homologous chromosomes during meiotic prophase are essential for correct segregation of chromosomes during meiotic divisions. Significant movements of chromosomes within the nucleus are required to achieve search and pairing of homologous chromosomes. Understanding mechanisms for proper movements of chromosomes is clinically important because chromosome missegregation during meiosis is a major cause of human miscarriage and developmental abnormalities (Hassold et al., 1996).

In many organisms, telomeres dramatically change their organization within the nucleus upon entering meiosis. While telomeres are dispersed along the nuclear envelope during the mitotic cell cycle, during meiotic prophase they form a cluster beneath the nuclear envelope to produce a characteristic bundled configuration of chromosomes, which is called the "bouquet" arrangement (reviewed by Scherthan, 2001). This widespread phenomenon of bouquet formation has implied a conserved role for telomeres in meiosis.

The fission yeast *Schizosaccharomyces pombe* exhibits a striking example of meiotic bouquet formation. In this organism, centromeres cluster near the SPB during the mitotic cell cycle (Funabiki et al., 1993); however, during meiotic prophase, centromeres detach from the SPB, and instead telomeres cluster next to the SPB (Chikashige et al., 1994). This reorganized nucleus also elongates and oscillates between the cell poles, mediated by cytoplasmic microtubules with cytoplasmic dynein as a microtubule motor protein (Ding et al., 1998; Yamamoto et al., 1999). The elongated nucleus is known as the "horsetail" nucleus, due to its characteristic shape. It has been demonstrated that telomere clustering and nuclear movement facilitate the alignment of homologous chromosomes and promote their pairing and recombination (Ding et al., 2004). Loss of telomere clustering or horsetail nuclear movement results in reduced homologous recombination and increased missegregation (Cooper, 2000; Yamamoto and Hiraoka, 2001). Thus, telomere clustering is an important initial step for chromosome movement during meiosis.

Both telomere and SPB integrity are necessary for normal formation of the meiotic bouquet. Taz1 and Rap1 are constitutive telomere-associated proteins in *S. pombe*. Taz1 is an ortholog of human TRF1 and TRF2 (Zhong et al., 1992; Bilaud et al., 1997; Broccoli et al., 1997), and directly binds to the telomeric repeat sequences (Cooper et al., 1997). Rap1, an ortholog of human RAP1 (Li et al., 2000), binds to the telomere through interaction

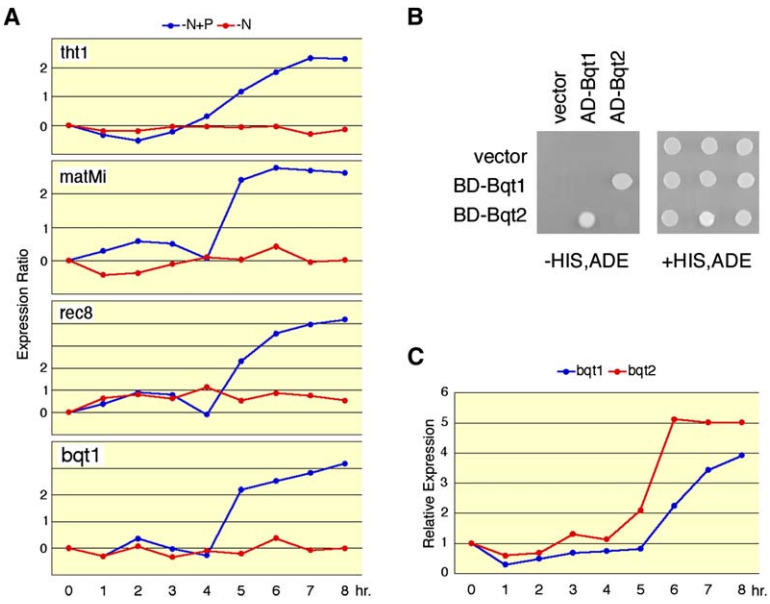

Figure 1. Meiotic Expressions of *bqt1* and *bqt2*

(A) The DNA microarray used contains 4,934 ORFs (Y. Chikashige and Y. Hiraoka, unpublished results; details will be published elsewhere). Examples of expression profile analyzed by DNA microarray experiments. Red indicates the case of nitrogen starvation only. Blue indicates the case of P-factor treatment with nitrogen starvation. Expression ratio (see Experimental Procedures) of each gene is plotted at each time point (hour) after nitrogen starvation and P factor treatment.

(B) Two-hybrid interaction of Bqt1 and Bqt2.

(C) The expression of Bqt2 is induced by P-factor as well as Bqt1.

with Taz1 (Chikashige and Hiraoka, 2001; Kanoh and Ishikawa, 2001). Loss of Taz1 or Rap1 leads to telomere elongation but does not affect mitotic cell growth; however, *rap1Δ* and *taz1Δ* strains display defects in meiosis with loss of telomere clustering (Cooper et al., 1998; Nimmo et al., 1998; Chikashige and Hiraoka, 2001; Kanoh and Ishikawa, 2001). On the other hand, Sad1 is essential for mitotic growth as a major constitutive component of the SPB (Hagan and Yanagida, 1995) and is a founding member of the SUN domain protein family (for Sad1 and Unc-84; Starr et al., 2001; Gruenbaum et al., 2005). Kms1 is another SPB component that affects integrity of the meiotic SPB. In the absence of Kms1, Sad1 forms multiple spots on the nuclear envelope in meiotic prophase, and telomeres fail to cluster while they associate with the Sad1 foci (Shimanuki et al., 1997). Similar multiple spots of Sad1 and loss of telomere clustering are also observed in *dot* mutants (Jin et al., 2002).

It remains unclear how telomeres specifically associate with the SPB during meiosis. A physical interaction between Ccq1 and the SPB protein Pcp1 has been proposed to link telomeres to the SPB (Flory et al., 2004), yet these proteins are also expressed but do not colocalize in vegetatively growing cells. Because meiotic telomere clustering is specifically induced by the mating pheromone response in *S. pombe* and not by nitrogen starvation (Chikashige et al., 1997; Yamamoto et al., 2004), we reasoned that telomere-SPB connectors might be found among the proteins that are expressed in response to mating pheromone signaling. Our genome-wide search identified two novel proteins, Bqt1 and Bqt2, that connect telomeres to the SPB when mating pheromone signaling is induced in meiosis. Neither Bqt1 nor Bqt2 alone functions as a connector, but the two proteins together form a bridge between Rap1 and Sad1. Thus, cooperation between Bqt1 and Bqt2 is essential for connecting telomeres to the SPB.

RESULTS

A Genome-Wide Search Identified Two Novel Proteins Required for Telomere Clustering

To find telomere-SPB connectors, we selected candidate genes that are expressed specifically under mating pheromone signaling based on gene expression profiles in DNA microarray data (see Experimental Procedures). We first selected 160 genes whose expression required mating pheromone signaling and was not observed under nitrogen starvation in the absence of mating pheromone. These included well-known meiotic genes, i.e., *tht1*$^+$, *rec8*$^+$, and the mating-type genes (Figure 1A). A complete list of these genes is provided in Table S1. By excluding well-characterized genes, we narrowed this list to 105 candidate genes. We then systematically disrupted each of these genes in an *S. pombe* strain expressing Taz1-GFP as a fluorescent marker for the telomere; 83 strains disrupted specific genes were successfully generated. All of these gene-disrupted strains showed normal mitotic growth as expected from the meiosis-specific expression of these genes. These strains were microscopically observed for telomere clustering in meiotic prophase, and one of the strains showed loss of telomere clustering (Figure 2A). We named this gene *bqt1* for "*b*ouquet" formation.

We identified a second gene by yeast two-hybrid screening using Bqt1 as a bait. For this screen, we constructed a library of cDNAs expressed in response to mating pheromone (see Experimental Procedures). The result of two-hybrid assay is shown in Figure 1B. Because disruption of this interacting gene also caused loss of the bouquet formation in meiotic prophase (Figure 2A), we named it *bqt2*. Although the *bqt2* gene was not included among the initial 160 candidates, analysis of gene expression by a real-time PCR method showed that expression of *bqt2* as well as that of *bqt1* was induced under

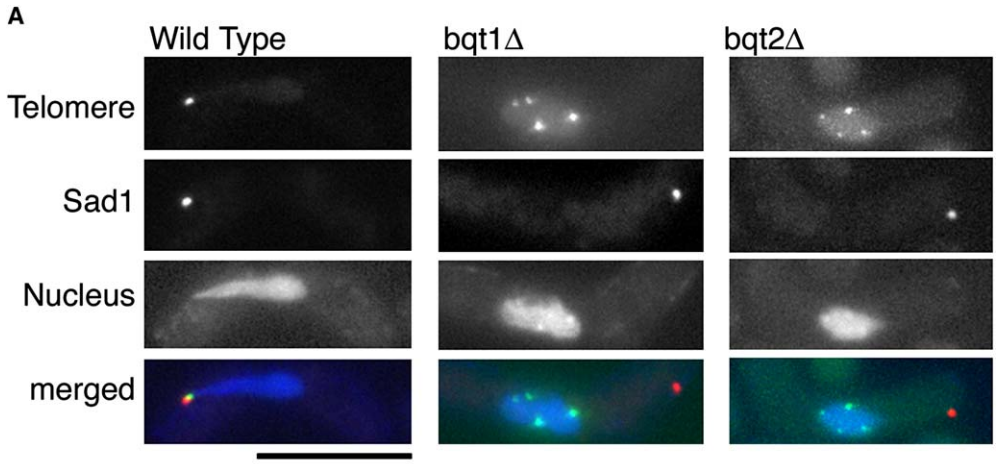

D

Genetic marker		Genetic distance	Numbers of tetrads		Rand0m spore analysis
		cM	PD:TT:NPD	Total	% (Non-parental/Total)
lys3 x ura1	WT x WT	16	50:24:0	74	22.5 (79/351)
	bqt1Δ x bqt1Δ	4.2	92: 2:1	95	3.1 (10/321)
his2 x leu1	WT x WT	9.7	88:14:1	103	11.7 (43/368)
	bqt2Δ x bqt2Δ	3.4	96: 7:0	103	2.3 (7/305)

Figure 2. Phenotypes of *bqt1Δ* and *bqt2Δ* Cells

(A) Loss of telomere clustering in *bqt1Δ* and *bqt2Δ* cells. Cells expressing both Taz1-GFP (green in the merged pictures) and Sad1-mRFP (red in the merged pictures) were observed after induction of meiosis (see Experimental Procedures). Nucleus was counterstained by Hoachst33342 (blue in the merged pictures). Failure in telomere-SPB cluster formation was found in all cases (30 for *bqt1Δ*, 52 for *bqt2Δ*) examined. Bar indicates 10 μm. Observed strains shown here are CRLi50 (wild-type), CRLi49 (*bqt1Δ*), and CRLj33 (*bqt2Δ*).

(B) Phase contrast images of asci with defects in spore formation.

(C) Spore formation and spore viability. Normal four-spore formation (%) = 100 × (number of asci containing normal four spores)/(number of asci dissected randomly). Spore viability (%) = 100 × (number of viable spores)/(4 × [number of asci dissected randomly]). Strains used here were CRLg80 (wild-type), CRLg50 (*bqt1Δ*), and CRLj39 (*bqt2Δ*).

(D) Tetrads analysis of genetic linkage. Genetic distance = 50(TT + 6NPD)/total number of asci. Strains used in the tetrads analysis were CRLg48 × CRLh20, CRLg11 × CRLg27, CRL168 × CRL191, CRLi55 × CRLi99. In random spore analysis, the number of nonparental segregants was divided by the total number of viable spores dissected.

mating pheromone signaling (Figure 1C). While Bqt1 and Bqt2 have been annotated as hypothetical proteins (SPAC6G9.13c and SPAC1002.06c, respectively), which were predicted to encode 101 and 118 amino acid sequences in the *S. pombe* genome database (Wood et al., 2002), here we confirmed that these genes are indeed expressed during meiosis. Full-length cDNAs were isolated and revealed that *bqt1* and *bqt2* encode 132 and 118 amino acid proteins (accession numbers AB232930 and AB232931), respectively (an extra exon was found in *bqt1*, extending it to 132 residues).

Although no obvious homologs of Bqt1 or Bqt2 were found, Bqt1 shares a weak sequence similarity with the fungal centromere protein Dam1 (Figures S1A–S1C), which is localized at the kinetochore during mitosis and plays a role in miotic spindle attachment (Westermann et al., 2005). Interestingly, fusion of Bqt1 to the C terminus of Bqt2 illuminated a sequence similarity with *S. cerevisiae* Spo74, which is known as a meiosis-specific SPB component (Nickas et al., 2003) (Figure S1D). We also found that the promoters of the *bqt1*$^+$ and *bqt2*$^+$ genes share Mlu1 cell cycle box (MCB) motifs. It is known that several genes that contain MCB motifs in their promoter regions are regulated during premeiotic S-phase. Expression of these genes, including *rec8*$^+$, *rec11*$^+$, *cdc18*$^+$, and *cdc22*$^+$, during premeiotic S-phase is regulated by the DNA

synthesis control-like transcription factor complex (DSC1) acting on MCB motifs (Cunliffe et al., 2004). Our analysis by DNA microarray revealed that expression of these genes as well as *bqt1*$^+$ and *bqt2*$^+$ is induced by mating pheromone signaling (Table S1). Thus, DSC-MCB regulation also seems to act downstream of mating pheromone signaling.

Bqt1 and Bqt2 Connect Telomeres to the SPB

To characterize the functions of Bqt1 and Bqt2, we examined the phenotypes of *S. pombe* cells disrupted for the *bqt1* or *bqt2* gene (*bqt1Δ* and *bqt2Δ*, respectively). As expected from their meiosis-specific expression, cells of the *bqt1Δ* and *bqt2Δ* strains were viable during mitotic cell growth. However, as shown in Figure 2A, both strains were defective in telomere clustering to the SPB during meiotic prophase, as their telomeres were scattered in the horsetail nucleus. Time-lapse observations showed that telomeres never formed a cluster during the entire period of the horsetail stage (Figures S2 and S3). Thus, we concluded that both Bqt1 and Bqt2 are required for clustering telomeres at the SPB. These strains also showed defects in spore formation and spore viability (Figures 2B and 2C). These defects in *bqt1Δ* and *bqt2Δ* cells likely reflect chromosome segregation errors as seen in Figures S2 and S3. Recombination frequency, which was determined by tetrad analysis using four viable spores, decreased moderately (3- to 4-fold) (Figure 2D). These values for reduction are comparable to other characterized mutants defective in telomere clustering such as *taz1Δ* or *rap1Δ* (Cooper et al., 1998; Nimmo et al., 1998; Cooper, 2000; Chikashige and Hiraoka, 2001; Kanoh and Ishikawa, 2001). Taken together, loss of Bqt1 or Bqt2 does not affect mitotic cell growth but causes defects in meiotic telomere clustering, meiotic recombination, and spore formation.

Next, we examined subcellular localization of Bqt1 and Bqt2. During meiosis, Bqt1-GFP formed a single spot in the horsetail nucleus, which was colocalized with Taz1 at the telomere and with Sad1 at the SPB (Figure 3A), indicating that Bqt1 was localized at the site of the telomere-SPB cluster. Bqt2 was also localized at the site of the telomere-SPB cluster in the horsetail nucleus as it was colocalized with Taz1 at the telomere and with Sad1 at the SPB (Figure 3C). Time-lapse observations showed that Bqt1 and Bqt2 were colocalized with the telomere cluster throughout the horsetail stage and disappeared before the first meiotic division when telomeres declustered (Figure S4). To test if the localization of Bqt1 depends on Bqt2, we examined Bqt1 localization in *bqt2Δ* cells. In the absence of Bqt2, telomeres are scattered, as shown in Figure 2A. In these *bqt2Δ* cells, Bqt1 still formed a single spot and was colocalized exclusively with Sad1 at the SPB (Figure 3B). Thus, we concluded that Bqt1 localized at the SPB, but not at the telomeres, in the absence of Bqt2. In the absence of Bqt1, Bqt2-GFP showed diffuse staining throughout the nucleus and was not localized at the telomere nor at the SPB (Figure 3D), indicating that Bqt2 localization at either the telomere or the SPB requires Bqt1.

Yeast two-hybrid assays consistently showed that Bqt1 directly bound to Sad1, whereas Bqt2 did not (Figure 4A). On the other hand, neither Bqt1 nor Bqt2 alone interacted with Rap1, but Bqt1 interacts with Rap1 in the presence of Bqt2 and vice versa (Figure 4B). Interactions of Bqt1 or Bqt2 with Taz1 were not detected under the same conditions (Figure 4B). Coimmunoprecipitation also showed that interaction between Rap1 and Bqt2 requires Bqt1 (Figure 4C). Taken together, these results showed that Bqt1 directly binds to Bqt2 and to Sad1 and that Bqt2 binds to Sad1 through interaction with Bqt1. Either Bqt1 or Bqt2 alone does not bind to Rap1, but they bind to Rap1 when both are present.

Expression of Bqt1 and Bqt2 in Mitotic Cells Recruit Sad1 to the Telomere

Since Bqt1 and Bqt2 form direct physical interactions with a telomere component, Rap1, and a SPB component, Sad1, we tested whether these proteins are sufficient to form a physical link between telomeres and the SPB if they are artificially expressed in mitotic cells. When Bqt1 alone was expressed in mitotic cells, a single spot of Sad1 was observed while Rap1 was localized at multiple sites of the telomere, as in wild-type cells. Bqt1 colocalized with Sad1 but not with Rap1 (Figure 4D). When Sad1 was overexpressed in these cells, the protein was observed along to the nuclear envelope rather than just at the SPB, and Bqt1 was also observed at the nuclear envelope (Figure 4E), which might be expected based on interaction between Bqt1 and Sad1. Thus, Bqt1 alone associates with Sad1 but is not sufficient to connect Sad1 to Rap1. On the other hand, when Bqt2 alone was expressed in mitotic cells, Bqt2 was diffuse in the nucleus and colocalized with neither Sad1 nor Rap1 (data not shown). In contrast, when both Bqt1 and Bqt2 were expressed in mitotic cells, Sad1 was observed at multiple sites where Bqt1 was colocalized with Sad1 and Rap1 (Figure 4F). In addition, fluorescence in situ hybridization experiments confirmed that telomeric DNA sequences were colocalized with Sad1 (Figure S5B). Thus, Bqt1 and Bqt2 together recruit Sad1 to Rap1 bound telomeres. These results are consistent with the results of localization in meiotic cells and also with the results of interactions examined by yeast two-hybrid assay. Therefore, we concluded that Bqt1 and Bqt2 are sufficient to form a bridge between Rap1 and Sad1.

Sad1 Bound Telomeres Are Tethered to the SPB in Meiotic Prophase

To better understand the dynamics of telomere clustering during meiosis, we carried out real-time analysis of this process in living cells. In particular, we were intrigued by the fact that Sad1 protein is usually observed as a single focus during meiotic prophase, but in several mutant backgrounds, including as *kms1* and *dot2*, multiple spots of Sad1 are detected (Shimanuki et al., 1997; Jin et al.,

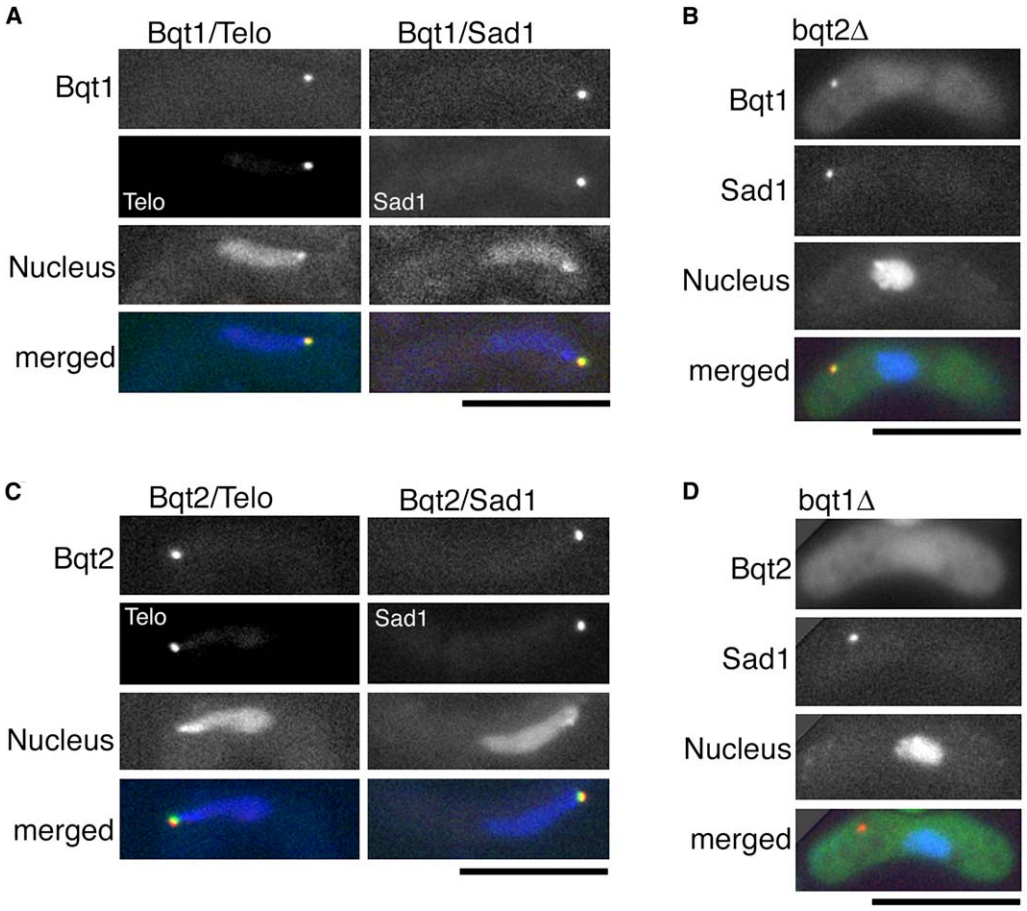

Figure 3. Localization of Bqt1 and Bqt2 in Horsetail Nucleus

(A and C) Cells expressing Bqt1-GFP or Bqt2-GFP (green in the merged pictures) and Sad1-mRFP or Taz1-mRFP (red in the merged pictures) were observed after induction of meiosis. Nucleus was counterstained by Hoachst33342 (blue in the merged pictures). Complete colocalization Bqt1 and telomeres were found in 36 out of 45 cases (CRLi71) examined (80%). Complete colocalization of Bqt1 and Sad1 were found in 30 out of 40 cases (CRLj10) examined (75%). Complete colocalization of Bqt2 and telomeres were found in 37 out of 43 cases (CRLj40) examined (86%). Complete colocalization of Bqt2 and Sad1 were found in 18 out of 20 cases (CRLi83) examined (90%). Because telomere clustering was recovered in these cells, functionality of Bqt1-GFP and Bqt2-GFP was confirmed.

(B and D) Cells, in which both *bqt1*$^{+}$ and *bqt2*$^{+}$ were disrupted, expressing GFP-Bqt1 or Bqt2-GFP with Sad1-mRFP were observed after induction of meiosis. GFP-Bqt1 or Bqt2-GFP was expressed by nmt1 promoter before induction of meiosis (see Experimental Procedures). Complete colocalization of Bqt1 and Sad1 were found in 23 out of 25 cases (CRLj18) examined (92%). Defused Bqt2 was observed in 18 out of 22 cases (CRLj20) examined (82%). Bar indicates 10 μm.

2002). To investigate the significance of the multiple Sad1-foci in mutant cells, we carried out time-lapse imaging of living meiotic cells expressing both Rap1-GFP and Sad1-mRFP (Figure 5A). In these experiments, we induced meiosis synchronously in *pat1-114* cells as described in Chikashige et al. (2004). In Figure 5A, initially a single spot of Sad1 was observed, and multiple telomere spots were separated from the Sad1 spot (89 min); then Sad1 appeared at multiple additional spots colocalized with telomeres (109 min and 139 min; indicated by the arrow). The Sad1 spot that is not colocalized with Taz1 is presumebly the SPB (109 min). Finally, Sad1 again formed a single spot together with telomeres (180 min). These results illustrate that Sad1 is initially associated with the SPB, then transiently redistributed to multiple sites of Rap1-bound telomeres, and eventually concentrated again at the SPB as telomeres become clustered. Thus, the appearance of multiple Sad1 foci reflects an intermediate state of telomere clustering that occurs during the normal process of meiosis. This dispersal of Sad1 to multiple telomere foci is a reminiscence of the Sad1distribution observed in mitotic cells ectopically expressing Bqt1 and Bqt2 (Figure 4F). However, the clustering of Sad1 bound telomeres at the SPB occurs in meiotic cells but apparently not in mitotic cells expressing Bqt1 and Bqt2 (Figures 4F and 5A). Meiotic clustering of Sad1 foci to the SPB is likely mediated by Kms1, which interacts with microtubule motor proteins, since loss of Kms1 results in persistent multiple foci of Sad1 (Figure 5C; see Discussion).

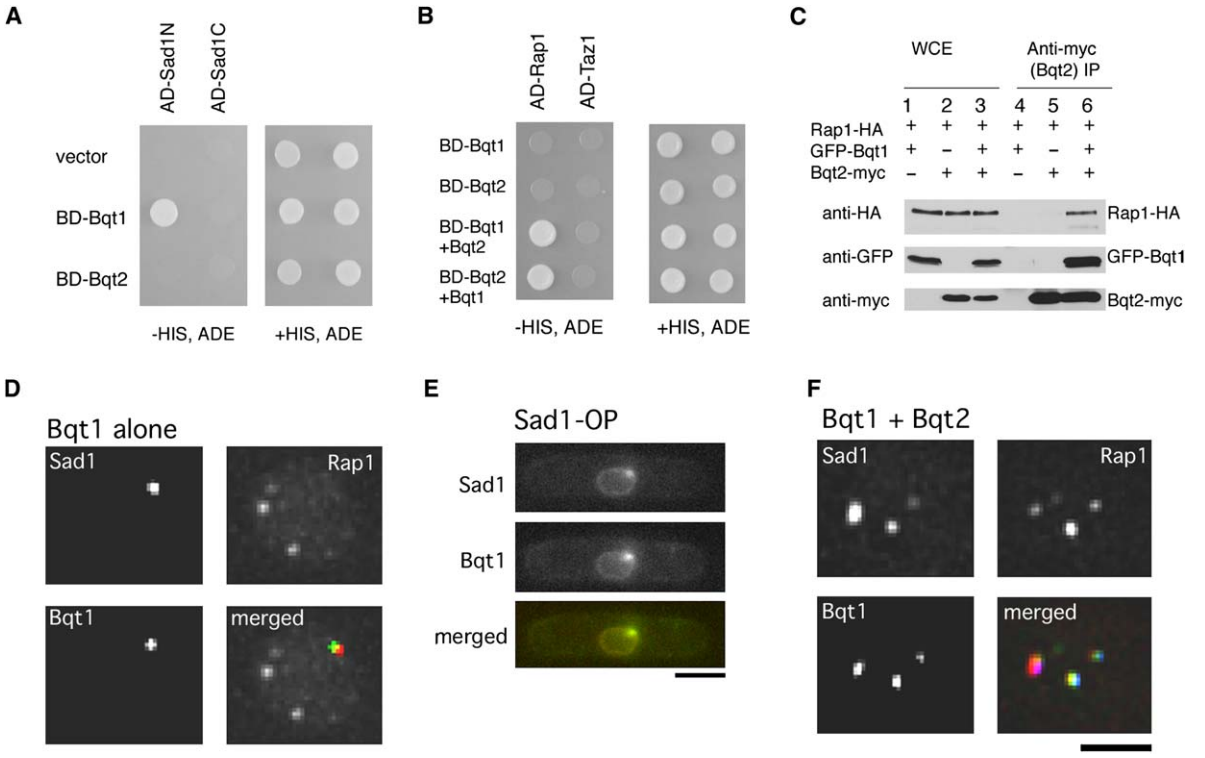

Figure 4. Interactions of Bqt1, Bqt2, Sad1, and Rap1

(A) Two-hybrid interaction of Bqt1 and Sad1-N. Sad1-N contains 169 aa to the N-terminal, excluding the transmembrane helix. Sad1-C contains 326 a.a. to the C-terminal, excluding the transmembrane helix.

(B) Three-hybrid interaction of Bqt1, Bqt2, and Rap1.

(C) Immunoprecipitation of Bqt2 and Rap1 in mitotic cells in the presence or absence of Bqt1. Strains used are CRLk60 (lanes 1 and 4), CRLk59 (lanes 2 and 5), and CRLk63 (lane 3 and 6).

(D) Localization of Bqt1 (CFP), Sad1 (mRFP), and Rap1(GFP) in mitotic cells (CRLk88) in which Bqt1 is expressed. In these cells, Sad1 showed a single dot colocalized with Bqt1, and this single dot of Sad1 was separated from Rap1 foci: Only one out of 65 Sad1 foci counted in 61 cells was colocalized with Rap1.

(E) Bqt1 is colocalized with overproduced Sad1 on the nuclear envelope. The strain observed is CRLk44.

(F) Localization of Bqt1 (CFP), Sad1(mRFP), and Rap1(GFP) in mitotic cells (CRLk42) in which both Bqt1 and Bqt2 are expressed. In most of these cells, Sad1 showed multiple foci colocalized with Bqt1, and many of these Sad1 foci were colocalized with Rap1: 116 out of 138 Sad1 foci counted in 80 cells were colocalized with Rap1. Those cells were observed 16 hr after induction of Bqt1 and Bqt2. No mitotic defects were observed under these conditions, although prolonged induction (3–4 days on a plate without thiamine) of Bqt1 and Bqt2 in mitotic cells caused some abnormal phenotypes of cell elongation and/or multiple septa in a small fraction of the cells (Figure S5A). Bar indicates 2 μm.

DISCUSSION

A genome-wide search identified two meiosis-specific protein components, Bqt1 and Bqt2, that are necessary for meiotic bouquet formation. Upon expression of Bqt1 and Bqt2 induced by mating pheromone signaling in meiosis, Sad1 is recruited to Rap1 bound telomeres through interaction with Bqt1 and Bqt2. Subsequently, Sad1 bound telomeres are tethered to the SPB. Significantly, when both Bqt1 and Bqt2 are ectopically expressed in mitotically growing cells, Sad1 accumulates at sites of Rap1-bound telomeric foci at the nuclear envelope. Our results demonstrate that Bqt1 and Bqt2 together form a bridge between Sad1 and Rap1: Bqt1 binds to Sad1, Bqt2 bind to Bqt1, and a complex of Bqt1 and Bqt2 binds to Rap1. Consistent results were obtained using three independent experimental approaches, analysis of intracellular localization in live meiotic prophase cells, analysis of molecular interactions by two hybrid assays or coimmunoprecipitation, and ectopic expression in mitotic cells. Therefore, we conclude that Bqt1 and Bqt2 are necessary and sufficient to connect telomeric Rap1 to Sad1 on the nuclear envelope. Furthermore, our results pinpoint Sad1 as the specific SPB component that interacts with telomeres during meiosis.

Architecture of the Telomere-SPB Complex within the Nuclear Membranes

Figure 5C illustrates a detailed model for the architecture of the telomere-Sad1 complex at the nuclear envelope. The nuclear envelope is composed of inner and outer nuclear membranes as well as a network of proteins, some of

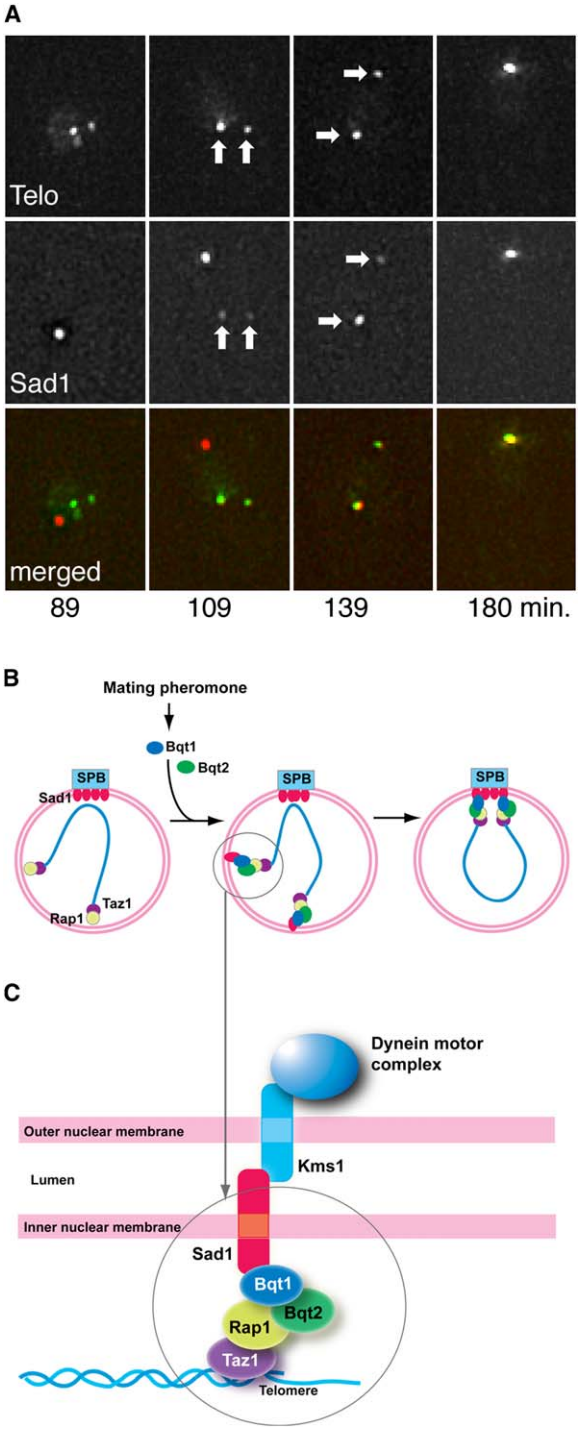

Figure 5. Clustering of Sad1-Associated Telomeres to the SPB

(A) Diploid *pat1-114* cells expressing Sad1-mRFP and Taz1-GFP (CRLh04) were observed during meiosis induced by shifting the temperature to 34°C, following nitrogen starvation. Time-lapse images were recorded at intervals of about 10 min, starting at 38 min after the temperature shift. Selected images are shown, and complete series of time-lapse images throughout the horsetail stage are shown in Figure S6. Numbers on the bottom of each image indicate the time after the temperature shift in minutes. An image at each time point is a projection of optical section images taken in three dimensions. In 89 of 94 cells examined, a single spot of Sad1 protein was scattered to form multiple foci; in five cells, only one spot of Sad1 was detected throughout the horsetail stage. In all of the 89 cells with multiple Sad1 foci, at least one of these Sad1 foci showed association with the telomere (Taz1) during the horsetail stage.

(B) During mitosis, telomeres are located near the nuclear membrane, and Sad1 is exclusively localized at the SPB. When induced by mating pheromone signaling, Bqt1 and Bqt2 connect Sad1 to Rap1 at the telomeres on the nuclear membrane; Sad1 bound telomeres are then tethered to the SPB along cytoplasmic microtubules by the dynein motor complex that interact with Sad1 bodies.

(C) Architecture of the telomere-SPB complex. The nuclear envelope is composed of inner and outer nuclear membranes. Sad1 in the inner nuclear membrane interacts with Bqt1 at the nucleoplasmic side. Sad1 interacts with Kms1 in the lumen. Kms1 in the outer nuclear membrane interacts with a dynein complex at the cytoplasmic side. Taz1 directly binds to telomeric DNA repeats, and Rap1 binds to the telomere through interaction with Taz1. Sad1 interacts with Kms1, which interacts with the dynein motor complex. Bqt1 binds to Sad1 directly and to Rap1 in the presence of Bqt2. Thus, in the presence of Bqt1 and Bqt2, Rap1 is connected to Sad1.

which are anchored in the membranes by transmembrane domains. Sad1 contains a single transmembrane domain, similarly to other SUN domain proteins that localize to the nuclear envelope (Starr et al., 2001). We found that the N terminus of Sad1 interacts with Bqt1 at the telomere in yeast two-hybrid assays (Figure 4A), in which interactions occurring in the nucleoplasm are monitored, suggesting that Sad1 is embedded in the inner nuclear membrane with its N terminus oriented on the nucleoplasmic side and C terminus in the lumen. We expect that Kms1 is embedded in the outer nuclear membrane because Kms1 interacts with dynein light chain (Dlc1), a component of the dynein motor complex, on the cytoplasmic side (Miki et al., 2002). As it is known that Sad1 interacts with Kms1 (Miki et al., 2004), it is likely that this interaction occurs in the lumen. Here we found that Sad1 interacts with Rap1 through interaction with Bqt1 and Bqt2. Thus, the meiosis-specific expression of Bqt1 and Bqt1 connects telomeres to the dynein motor complex through the nuclear envelope. This connection to the dynein motor complex can explain the driving forces for clustering telomeres.

Sad1-Mediated Movements of Chromosomes across the Nuclear Membranes

Our live cell observations during meiotic prophase showed that multiple foci of Sad1 appeared transiently, as an intermediate stage in the clustering of telomeres to the SPB (Figure 5A). Accumulation of Sad1 at multiple sites of Rap1 bound telomeres on the nuclear envelope was also observed when Bqt1 and Bqt2 are ectopically expressed in mitotically growing cells (Figure 4F). Thus, Bqt1 and Bqt2 are sufficient to mediate a link between Sad1 and Rap1 at the telomere. However, in mitotic cells, these Sad1 bodies do not form a single cluster. These results indicate that clustering of telomeres requires activities that cannot be provided solely by expression of

Table 1. List of Strains Used

L972	h-
CRLg80	h90, leu1-32, lys1+::LEU2
CRLg48	h+, his2-245, leu1-32, lys1+::LEU2
CRLh20	h-, leu1-32, lys1+::LEU2, lys3, ura1
CRL168	h-, leu1-32, lys1-131, ade6-210
CRL191	h+, his2-245, lys1-131, ade6-216
CRLg11	h+, his2-245, leu1-32, bqt1D::LEU2
CRLg27	h-, leu1-32, lys3, ura1, bqt1D::LEU2
CRLi55	h-, leu1-32, lys1-131, ura4-D18, ade6-216, bqt2D::ura4+
CRLi99	h+ his2-245, lys1-131, ura4-D18, ade6-210, bqt2D::ura4+
CRLg50	h90, leu1-32, bqt1D::LEU2
CRLj39	h90, lys1-131, ura4-D18, bqt2D::ura4+
CRLh04	h-/h-, leu1-32/+, lys1+::taz1-GFP/lys1+::taz1-GFP, ura4-D18/ura4-D18, ade6-210/ade6-216, taz1D::ura4+/taz1D::ura4+, sad1-mRFP::kan/+, pat1-114/pat1-114
CRL672	h-, ura4-D18, sxa2D::ura4+
CRL682	h90, leu1-32, lys1+::taz1-GFP, ura4-D18
CRL760	h90, leu1-32, lys1+::taz1-GFP, ura4-D18, ade6-210, taz1D::ura4+
CRLi50	h90, leu1-32, lys1+::taz1-GFP, ura4-D18, ade6-210, taz1D::ura4+, sad1-mRFP::kan
CRLi49	h90, leu1-32, lys1+::taz1-GFP, ura4-D18, ade6-210, taz1D::ura4+, sad1-mRFP::kan, bqt1D::LEU2
CRLj33	h90 leu1-32, lys1-131, ura4-D18, ade6-216, rap1-GFP::LEU2, sad1-mRFP::kan, bqt2D::ura4+
CRLi71	h90 leu1-32, lys1+::taz1-mRFP, ura4-D18, ade6-210, taz1D::ura4+, bqt1-GFP::kan
CRLj10	h90 leu1-32, lys1-131, ura4-D18, ade6-216, sad1-mRFP::kan, bqt1-GFP::kan
CRLj40	h90 leu1-32, lys1+::taz1-mRFP, ura4-D18, ade6-210, taz1D::ura4+, bqt2-GFP::kan
CRLi83	h90 leu1-32, lys1-131, ura4-D18, ade6-210, sad1-mRFP::kan, bqt2-GFP::kan
CRLj18	h90 leu1-32, lys1+::nmt1-GFP-bqt1, ura4-D18, ade6-210, sad1-mRFP::kan, bqt1D::LEU2, bqt2D::ura4+
CRLj20	h90 leu1-32, lys1+::nmt1-bqt2-GFP,:ura4+-D18, ade6-210, sad1-mRFP::kan, bqt1D::LEU2, bqt2D:::ura4+
CRLk42	h-/h-, leu1-32/leu1-32, lys1+::nmt1-bqt2-HA/lys1+::nmt1-CFP-bqt1, sad1-mRFP/+, rap1-GFP/+
CRLk88	h-/h-, leu1-32/leu1-32, lys1+::nmt1-CFP-bqt1/lys1-131, ura4-D18/ura4-D18, ade6-210/ade6-216, sad1-mRFP/+, rap1-GFP/+
CRLk43	h-/h-, leu1-32/leu1-32, lys1-131/lys1+::nmt1-GFP-bqt1, ura4-D18/+, ade6-210/ade6-216, sad1-mRFP/+
CRLk44	h-/h-, leu1-32/leu1-32, lys1+::nmt1-GFP-bqt1/lys1+::nmt1-sad1-mRFP, ura4-D18/ura4-D18, ade6-210/ade6-216
CRLk59	h- leu1-32, lys1-131, ura4-D18, ade6-216, bqt1D::LEU2, bqt2D::ura4+, rap1-HA::LEU2, aur1-r::nmt1-bqt2-myc
CRLk60	h- leu1-32, lys1+::nmt1-GFP-bqt1, ura4-D18, ade6-216, bqt1D::LEU2, bqt2D:::ura4+, rap1-HA::LEU2
CRLk63	h- leu1-32, lys1+::nmt1-GFP-bqt1, ura4-D18, ade6-216, bqt1D::LEU2, bqt2D:::ura4+, rap1-HA::LEU2, aur1-r::nmt1-bqt2-myc
CRLk64	h- leu1-32, lys1+::nmt1-GFP-bqt1, ura4-D18, ade6-216, bqt1D::LEU2, bqt2D:::ura4+, aur1-r::nmt1-bqt2-myc

Bqt1 and Bqt2. Bouquet formation probably also involves meiosis-specific microtubule organization and motor activities, as it has been shown that upon entering to meiosis, cytoplasmic microtubules are significantly reorganized (Hagan and Hyams, 1988; Svoboda et al., 1995; Ding et al., 1998), and dynein motor proteins are expressed (Yamamoto et al., 1999; Miki et al., 2002). Kms1 is a likely candidate for tethering Sad1 foci to the SPB, as multiple telomere-associated Sad1 foci persist at the nuclear envelope in the absence of Kms1 (Shimanuki et al., 1997). A plausible model is that upon induction of Bqt1 and Bqt2 under mating pheromone signaling,

telomeres are connected to the Sad1 bodies on the nuclear envelope and are tethered to the SPB by Kms1 through interaction with the dynein motor complex on cytoplasmic microtubules.

Our conclusion that the conserved SUN domain of Sad1 at the C terminus is likely involved in microtubule-mediated telomere movements is supported by findings in other eukaryotic organisms demonstrating that SUN domain proteins provide a mechanism that links nuclear structures to the cytoskeleton (reviewed in Starr and Han, 2003). *C. elegans* Unc-84, a member of the SUN domain protein families, mediates migration of the nucleus during embryonic development (Starr et al., 2001). Furthermore, *C. elegans* SUN-1 and ZYG-12 mediate attachment between the centrosome and nucleus through dynein-mediated motility along microtubules (Malone et al., 2003). SUN-1 is thought to be embedded in the inner nuclear membrane and ZYG-12 in the outer nuclear membrane in a situation analogous to Sad1 and Kms1, respectively, in *S. pombe*.

Here we demonstrated that *S. pombe* Sad1, with Bqt1 and Bqt2 acting as a connector, mediates movements of telomeres inside the nucleus. Sad1-mediated chromosome movements along the nuclear envelope have also been observed when meiotically arrested cells return to mitotic growth: While scattered centromeres recluster to the SPB during this return-to-growth process, Sad1 and Kms1 are colocalized with the scattered centromeres (Goto et al., 2001). Thus, similar mechanisms of Sad1-mediated chromosome movements appear to act on the centromere as well. These findings demonstrate that Sad1 and possibly SUN domain proteins in general are capable of moving specific chromosomal loci along nuclear membranes by linking the cytoskeletal network to chromosomes via developmentally expressed connector proteins such as Bqt1 and Bqt2.

EXPERIMENTAL PROCEDURES

Strains, Culture Media, and Induction of Meiosis

Genotypes of the strains used in this paper are shown in Table 1. YE, YES, or EMM2 was used for routine mitotic culture of *S. pombe* cells, and ME agar plate was used for meiosis of h^{90} cells as described previously (Moreno et al., 1991). Wild-type h^{90} cells grown in a liquid medium were transferred to an ME plate at 26°C to induce meiosis, and the horsetail stage was observed at 12–16 hr after induction of meiosis. Live observations of meiosis induced by the pat1-114 mutation were described previously (Chikashige et al., 2004). Spore formation was examined 3 days after induction of meiosis.

DNA Microarray Experiments

We produced DNA microarrays by spotting PCR products corresponding to 4934 known and predicted *S. pombe* open reading frames onto glass slides. Detailed protocols for array production and analysis will be published elsewhere.

For RNA preparation, a single colony of *S. pombe* cells on a YES plate was inoculated into YES liquid medium to grow to 5×10^6 cell/ml at 30°C. After two washes in EMM2-N (EMM2 depleted of nitrogen sources), cells were transferred to EMM2-N with or without 0.5 μg/ml synthetic P-factor (Imai and Yamamoto, 1994) and further incubated at 30°C. Strains used were L972 for nitrogen starvation without P-factor and CRL672 (h- sxa2Δ) for nitrogen starvation with P-factor (see Table 1). Cells were collected at each time point after the nitrogen starvation. Total RNA was isolated by acid phenol methods described in http://www.sanger.ac.uk/PostGenomics/S_pombe/, and then polyA-RNA was purified by Oligotex-dT30<super>mRNA purification kit (Takara). The polyA-RNA (3–6 μg) was labeled by CyScribe Post-Labeling Kit (Amasham Pharmacia) with Cy3 or Cy5 with Oligo dT primer. The labeled targets are purified with GFX column (Amasham Pharmacia). It was confirmed that the difference of the incorporation ratio of Cy3 and Cy5 was within ±10%. The labeled targets were added to the hybridization solution to contain an equal amount of the Cy3 and Cy5 and then were hybridized onto DNA on the microarray using Genomic solutions GeneTac Hybridization Station for 4 hr at 40°C in Genomic solutions GeneTac Hyb buffer 120 μl (including 42% formamide). The slides after hybridization were washed in the following sequence: (1) 2 × SSC 0.1% SDS at 40°C for 5min; (2) 0.2 × SSC at 25°C for 1min; and (3) 0.1 × SSC at 25°C for 1min. Microarrays were scanned using an ArraywoRx arrayscanner, and the acquired data was analyzed by a SoftwoRx software (Applied Precision, Inc., Seattle, WA). Fluorescent intensity in each spot circle (150 μm diameter) was measured by Softworx tracker. In all microarray experiments shown here, RNA from vegetatively growing control cells were labeled with Cy3, and RNA from cells in each experimental condition were labeled with Cy5. Measured fluorescent intensity, I, was corrected as follows to give a corrected intensity, C:

$$C = I - M, \text{ (for } I \geqq M + 2s)$$
$$C = I * 2s/(M + 2s), \text{ (for } I \leqq M + 2s)$$

where M and s are an average and a standard deviation of I of negative control spots for each wavelength respectively. When I = M + 2s, that is C = 2s, it was set to be a detection limit. When C for either Cy3 or Cy5 or both were greater than 2s, the values were considered to be effective data. Expression ratio r' of the each effective detection spot obtained thus was scaled as follows: $r' = r - m$, $r = \log_2 R$, $R = (C_{cy5}/C_{cy3})$, m is an average of r of all effective detection spots. All microarray experiments were repeated twice. Average of expression ratios from repeated experiments are shown in Figure 2A. Original data of microarray experiments have been submitted to GEO (http://www.ncbi.nlm.nih.gov/geo/index.cgi; accession number GSE3515).

Disruption of Pheromone-Induced Genes

For gene disruption, we used either of the two selection markers, *S. cerevisiae* LEU2 and *S. pombe ura4*$^+$. CRL760 for LEU2 and CRL682 for *ura4*$^+$ were used as recipients. Gene disruption was done by PCR-based gene targeting methods (Krawchuk and Wahls, 1999). About 250 bp flanking DNA with homology to the target locus was generated by PCR. Primers used for gene disruption can be seen at http://www-karc.nict.go.jp/d332/CellMagic/index.html. Out of 160 genes upregulated by P-factor, we selected 105 function-unknown genes for disruption and obtained 83 disruptants out of them. A list of these 160 genes can be seen in Table S1.

Fluorescent Microscopy

Fluorescence microscope images were obtained by the DeltaVision microscope system (Applied Precision, Inc., Seattle, WA) and set up in a temperature-controlled room as described previously (Haraguchi et al., 1999).

Fluorescent Fusion Constructs

Strains carrying Bqt1-GFP, Bqt2-GFP, and Sad1-mRFP (monomeric RFP described in Campbell et al., 2002) were constructed by replacing the *bqt1*$^+$, *bqt2*$^+$, and *sad1*$^+$ genes respectively with a selection marker kan^r by a PCR-based gene targeting method (Bähler et al., 1998). Taz1-GFP and Taz1-mRFP fusion constructs were made as follows: The entire coding sequence of the *taz1*$^+$ gene with its own promoter region (Chikashige and Hiraoka, 2001) was ligated in-frame to the 5′-end

of the sequence encoding GFP-S65T or mRFP followed by the nmt1 terminator sequence, and it was then cloned into the integration vector pYC36 (Chikashige et al., 2004). The resulting plasmid was integrated into the chromosome at the *lys1* gene locus. Rap1-GFP and Rap1-HA were constructed as follows: The *rap1*$^+$ gene fused at its 3′-end with GFP-S65T or triple tandem HA epitope tags was integrated into the chromosome to replace the authentic *rap1*$^+$ gene using the *S. cerevisiae* LEU2 gene as a selection marker. Fusion construct under nmt1 promoter was made by using pCST3 (Chikashige et al., 2004) for integration at *lys1* locus. GFP-S65T, CFP, mRFP, and triple tandem HA epitope tags was inserted at BamHI-XhoI site of pCST3 to make pCST8, pCST101, p1093, and pCST2, respectively. For integration at *aur1* locus, the *aur1*^{R} gene was used to select Aureobasidin A resistant transformant (Takara). pCST159 was made by replacing lys1-N fragment of pCST3 with *aur1*^{R} gene. Quadruple tandem myc epitope tags were inserted at BamHI-XhoI site of pCST159 to make pCSU54. For ectopic expression of tagged genes with nmt1 promoter, pCST8, pCST101, p1093, pCST2, and pCSU54 were used. Restriction maps and DNA sequences of these integration vectors can be found at http://www-karc.nict.go.jp/d332/CellMagic/index.html.

Ectopic Expression of *bqt* Genes

For expression of GFP-Bqt1 and CFP-Bqt1, the full-length cDNA of *bqt1*$^+$ was inserted at BglII site of pCST8 and pCST101, respectively. The resulting plasmids were integrated into the chromosome at the *lys1* gene locus. For expression of Bqt2-HA and Bqt2-GFP, the full-length cDNA of *bqt2*$^+$ was inserted at BamHI site of pCST2 and pCST8, respectively. The resulting plasmids were integrated into the chromosome at the *lys1* gene locus. For expression of Bqt2-myc, the full-length cDNA of *bqt2*$^+$ was inserted at BamHI site of pCSU54. The resulting plasmid was integrated into the chromosome at the *aur1* gene locus. Transformants with tagged genes grown to 5×10^6 cell/ml in YES liquid medium were transferred to thiamine-removed EMM2 medium to induce the nmt1 promoter. After induction of the nmt1 promoter for four to five generations, the mitotic cells were observed.

Real-Time RT-PCR

Real-time PCR with TaqMan technology (ABI, Applied Biosystems) was used to measure the mRNA. When mRNA was measured, RNA was reverse-transcribed to cDNA by MultiScribe Reverse Transcriptase (ABI). Specific primers and TaqMan probes were designed with PrimereExpress software (ABI). Sequences of the primeres and TaqMan probes are TTGCTTTGCCAAGGTCAAAAT(bqt1-198F), GACA GAACTTACAATATCGTAGTTTGAAATT(bqt1-288R), FAM-ATCATTGA TACATATGGAAGAAGACGCCAGCA-TAMRA(bqt1-224T), CGAAATT TTTAGCAGAAGGTTATGAA(bqt2-19F), AACGACATTGAACTGATTT GTAATTTG(bqt2-120R), FAM-ATTATGCATTTTCAATGCATCTAAGA AAGCACGTC-TAMRA(bqt2-52T), CCACTGGTATCGTCTTGGACTCT (act1-243F), GCGAGATCAAGACGCATGATAG(act1-342R), FAM-CACTGTTCCCATTTATGAGGGTTATGCTCTTCC-TAMRA(act1-283T). A comparative threshold cycle (Ct) was used to determine gene expression relative to the vegetative growing phase using the $2^{-\Delta\Delta Ct}$ technique (ABI User Bulletin2), in which *act1*$^+$ was used as a endogenous reference.

Yeast 2- and 3-Hybrid Assay

Yeast 2-hybrid screening was carried out using BD Matchmaker library construction and screening kits. cDNA library for 2-hybrid screening was constructed from *S. pombe* cells (strain CRL672) treated with P-factor for 5–6 hr. For yeast 2-hybrid analysis, the BD MATCHMAKER GAL4 2-Hybrid System 3 (BD-Clontech) was used. The diploid cells carrying both pGADT7 and pGBKT7 plasmids were tested for expression of the two reporter genes (ADE2, HIS3) according to the BD MATCHMAKER system manual. For 3-hybrid assay, the plasmid pBridge (BD-Clontech) were used instead of pGBKT7.

Immunoprecipitation

Protein extracts were prepared as previously described (Tanaka et al., 2001). Strains used are CRLk60, CRLk59, and CRLk63 (Table 1); in these strains, fusion construct under nmt1 promoter is integrated into the chromosome. Cell extracts were prepared after induction of the nmt1 promoter for four to five generations. Immunoprecipitation was performed with anti-myc antibody (9E10; Santa Cruz Biotechnology, Inc., Santa Cruz, CA). Proteins from whole cell extracts and from precipitates were electrophoresed in SDS-polyacrylamide gels and immunoblotted with anti-HA (3F10, Roche), anti-myc (9E10), and anti-GFP (JL-8: BD-Clontech) antibodies.

Supplemental Data

Supplemental Data include six figures and one table and can be found with this article online at http://www.cell.com/cgi/content/full/125/1/59/DC1/.

ACKNOWLEDGMENTS

We thank Roger Y. Tsien for providing mRFP and Julia P. Cooper, Abby F. Dernburg, and Hirohisa Masuda for critical reading of the manuscript. We would especially like to thank Abby F. Dernburg for communicating their results prior to publication and for insightful discussion. This work was supported by grants from the Japanese Ministry of Education (MEXT) and the Japan Science and Technology Agency to T.H. and Y.H.

Received: September 7, 2005
Revised: December 14, 2005
Accepted: January 9, 2006
Published: April 6, 2006

REFERENCES

Bähler, J., Wu, J.Q., Longtine, M.S., Shah, N.G., McKenzie, A., 3rd, Steever, A.B., Wach, A., Philippsen, P., and Pringle, J.R. (1998). Heterologous modules for efficient and versatile PCR-based gene targeting in Schizosaccharomyces pombe. Yeast *14*, 943–951.

Bilaud, T., Brun, C., Ancelin, K., Koering, C.E., Laroche, T., and Gilson, E. (1997). Telomeric localization of TRF2, a novel human telobox protein. Nat. Genet. *17*, 236–239.

Broccoli, D., Smogorzewska, A., Chong, L., and de Lange, T. (1997). Human telomeres contain two distinct Myb-related proteins, TRF1 and TRF2. Nat. Genet. *17*, 231–235.

Campbell, R.E., Tour, O., Palmer, A.E., Steinbach, P.A., Baird, G.S., Zacharias, D.A., and Tsien, R.Y. (2002). A monomeric red fluorescent protein. Proc. Natl. Acad. Sci. USA *99*, 7877–7882.

Chikashige, Y., Ding, D.Q., Funabiki, H., Haraguchi, T., Mashiko, S., Yanagida, M., and Hiraoka, Y. (1994). Telomere-led premeiotic chromosome movement in fission yeast. Science *264*, 270–273.

Chikashige, Y., Ding, D.Q., Imai, Y., Yamamoto, M., Haraguchi, T., and Hiraoka, Y. (1997). Meiotic nuclear reorganization: switching the position of centromeres and telomeres in the fission yeast *Schizosaccharomyces pombe*. EMBO J. *16*, 193–202.

Chikashige, Y., and Hiraoka, Y. (2001). Telomere binding of the Rap1 protein is required for meiosis in fission yeast. Curr. Biol. *11*, 1618–1623.

Chikashige, Y., Kurokawa, R., Haraguchi, T., and Hiraoka, Y. (2004). Meiosis induced by inactivation of Pat1 kinase proceeds with aberrant nuclear positioning of centromeres in the fission yeast *Schizosaccharomyces pombe.* Genes Cells *9*, 671–684.

Cooper, J.P., Nimmo, E.R., Allshire, R.C., and Cech, T.R. (1997). Regulation of telomere length and function by a Myb-domain protein in fission yeast. Nature *385*, 744–777.

Cooper, J.P., Watanabe, Y., and Nurse, P. (1998). Fission yeast Taz1 protein is required for meiotic telomere clustering and recombination. Nature *392*, 828–831.

Cooper, J.P. (2000). Telomere transitions in yeast: the end of the chromosome as we know it. Curr. Opin. Genet. Dev. *10*, 169–177.

Cunliffe, L., White, S., and McInerny, C.J. (2004). DSC1-MCB regulation of meiotic transcription in Schizosaccharomyces pombe. Mol. Genet. Genomics *271*, 60–71.

Ding, D.Q., Chikashige, Y., Haraguchi, T., and Hiraoka, Y. (1998). Oscillatory nuclear movement in fission yeast meiotic prophase is driven by astral microtubules, as revealed by continuous observation of chromosomes and microtubules in living cells. J. Cell Sci. *111*, 701–712.

Ding, D.Q., Yamamoto, A., Haraguchi, T., and Hiraoka, Y. (2004). Dynamics of homologous chromosome pairing during meiotic prophase in fission yeast. Dev. Cell *6*, 329–341.

Flory, M.R., Carson, A.R., Muller, E.G., and Aebersold, R. (2004). An SMC-domain protein in fission yeast links telomeres to the meiotic centrosome. Mol. Cell *16*, 619–630.

Funabiki, H., Hagan, I., Uzawa, S., and Yanagida, M. (1993). Cell cycle-dependent specific positioning and clustering of centrosome and telomeres in fission yeast. J. Cell Biol. *121*, 961–976.

Goto, B., Okazaki, K., and Niwa, O. (2001). Cytoplasmic microtubular system implicated in de novo formation of a Rabl-like orientation of chromosomes in fission yeast. J. Cell Sci. *114*, 2427–2435.

Gruenbaum, Y., Margalit, A., Goldman, R.D., Shumaker, D.K., and Wilson, K.L. (2005). The nuclear lamina comes of age. Nat. Rev. Mol. Cell Biol. *6*, 21–31.

Hagan, I.M., and Hyams, J.S. (1988). The use of cell division cycle mutants to investigate the control of microtubule distribution in the fission yeast Schizosaccharomyces pombe. J. Cell Sci. *89*, 343–357.

Hagan, I., and Yanagida, M. (1995). The product of the spindle formation gene *sad1*$^{+}$ associates with the fission yeast spindle pole body and is essential for viability. J. Cell Biol. *129*, 1033–1047.

Haraguchi, T., Ding, D.Q., Yamamoto, A., Kaneda, T., Koujin, T., and Hiraoka, Y. (1999). Multiple-color fluorescence imaging of chromosomes and microtubules in living cells. Cell Struct. Funct. *24*, 291–298.

Hassold, T., Abruzzo, M., Adkins, K., Griffin, D., Merrill, M., Millie, E., Saker, D., Shen, J., and Zaragoza, M. (1996). Human aneuploidy: incidence, origin, and etiology. Environ. Mol. Mutagen. *28*, 167–175.

Imai, Y., and Yamamoto, M. (1994). The fission yeast mating pheromone P-factor: its molecular structure, gene structure, and ability to induce gene expression and G1 arrest in the mating partner. Genes Dev. *8*, 328–338.

Jin, Y., Uzawa, S., and Cande, W.Z. (2002). Fission yeast mutants affecting telomere clustering and meiosis-specific spindle pole body integrity. Genetics *160*, 861–876.

Kanoh, J., and Ishikawa, F. (2001). spRap1 and spRif1, recruited to telomeres by Taz1, are essential for telomere function in fission yeast. Curr. Biol. *11*, 1624–1630.

Krawchuk, M.D., and Wahls, W.P. (1999). High-efficiency gene targeting in Schizosaccharomyces pombe using a modular, PCR-based approach with long tracts of flanking homology. Yeast *15*, 1419–1427.

Li, B., Oestreich, S., and de Lange, T. (2000). Identification of human Rap1: implications for telomere evolution. Cell *101*, 471–483.

Malone, C.J., Misner, L., Le Bot, N., Tsai, M.C., Campbell, J.M., Ahringer, J., and White, J.G. (2003). The C. elegans hook protein, ZYG-12, mediates the essential attachment between the centrosome and nucleus. Cell *115*, 825–836.

Miki, F., Okazaki, K., Shimanuki, M., Yamamoto, A., Hiraoka, Y., and Niwa, O. (2002). The 14-kDa dynein light chain-family protein Dlc1 is required for regular oscillatory nuclear movement and efficient recombination during meiotic prophase in fission yeast. Mol. Biol. Cell *13*, 930–946.

Miki, F., Kurabayashi, A., Tange, Y., Okazaki, K., Shimanuki, M., and Niwa, O. (2004). Two-hybrid search for proteins that interact with Sad1 and Kms1, two membrane-bound components of the spindle pole body in fission yeast. Mol. Genet. Genomics *270*, 449–461.

Moreno, S., Klar, A., and Nurse, P. (1991). Molecular genetic analysis of fission yeast *Schizosaccharomyces pombe*. Methods Enzymol. *194*, 795–823.

Nickas, M.E., Schwartz, C., and Neiman, A.M. (2003). Ady4p and Spo74p are components of the meiotic spindle pole body that promote growth of the prospore membrane in Saccharomyces cerevisiae. Eukaryot. Cell *2*, 431–445.

Nimmo, E.R., Pidoux, A.L., Perry, P.E., and Allshire, R.C. (1998). Defective meiosis in telomere-silencing mutants of *Schizosaccharomyces pombe*. Nature *392*, 825–828.

Scherthan, H. (2001). A bouquet makes ends meet. Nat. Rev. Mol. Cell Biol. *2*, 621–627.

Shimanuki, M., Miki, F., Ding, D.Q., Chikashige, Y., Hiraoka, Y., Horio, T., and Niwa, O. (1997). A novel fission yeast gene, *kms1*$^{+}$, is required for the formation of meiotic prophase-specific nuclear architecture. Mol. Gen. Genet. *254*, 238–249.

Starr, D.A., Hermann, G.J., Malone, C.J., Fixsen, W., Priess, J.R., Horvitz, H.R., and Han, M. (2001). unc-83 encodes a novel component of the nuclear envelope and is essential for proper nuclear migration. Development *128*, 5039–5050.

Starr, D.A., and Han, M. (2003). ANChors away: an actin based mechanism of nuclear positioning. J. Cell Sci. *116*, 211–216.

Svoboda, A., Bähler, J., and Kohli, J. (1995). Microtubule-driven nuclear movements and linear elements as meiosis-specific characteristics of the fission yeasts Schizosaccharomyces versatilis and Schizosaccharomyces pombe. Chromosoma *104*, 203–214.

Tanaka, K., Hao, Z., Kai, M., and Okayama, H. (2001). Establishment and maintenance of sister chromatid cohesion in fission yeast by a unique mechanism. EMBO J. *20*, 5779–5790.

Westermann, S., Avila-Sakar, A., Wang, H.W., Niederstrasser, H., Wong, J., Drubin, D.G., Nogales, E., and Barnes, G. (2005). Formation of a dynamic kinetochore- microtubule interface through assembly of the Dam1 ring complex. Mol. Cell *17*, 277–290.

Wood, V., Gwilliam, R., Rajandream, M.A., Lyne, M., Lyne, R., Stewart, A., Sgouros, J., Peat, N., Hayles, J., Baker, S., et al. (2002). The genome sequence of Schizosaccharomyces pombe. Nature. *415*, 871–880. Erratum in:Nature (2003). *421*, 94.

Yamamoto, A., and Hiraoka, Y. (2001). How do meiotic chromosomes meet their homologous partners?: lessons from fission yeast. Bioessays *23*, 526–533.

Yamamoto, A., West, R.R., McIntosh, J.R., and Hiraoka, Y. (1999). A cytoplasmic dynein heavy chain is required for oscillatory nuclear movement of meiotic prophase and efficient meiotic recombination in fission yeast. J. Cell Biol. *145*, 1233–1249.

Yamamoto, T.G., Chikashige, Y., Ozoe, F., Kawamukai, M., and Hiraoka, Y. (2004). Activation of the pheromone-responsive MAP kinase drives haploid cells to undergo ectopic meiosis with normal telomere clustering and sister chromatid segregation in fission yeast. J. Cell Sci. *117*, 3875–3886.

Zhong, Z., Shiue, L., Kaplan, S., and de Lange, T. (1992). A mammalian factor that binds telomeric TTAGGG repeats in vitro. Mol. Cell. Biol. *12*, 4834–4843.

Note Added in Proof

Bqt1 and Bqt2 were independently identified as Rec26 and Rec23 in a screen for meiotic genes by Martin-Castellanos et al., (2005). Curr. Biol. *15,* 2056–2062. The gene names were unified to Bqt1 and Bqt2 based on personal communications.